Middlesex University Research Repository

An open access repository of

Middlesex University research

http://eprints.mdx.ac.uk

Copyright:

1

Optimising Energy Efficiency of NOMA for Wireless Backhaul in Heterogeneous CRAN

Quoc-Tuan Vien, Tuan Anh Le, Balbir Barn, Ca V. Phan

Abstract

This paper studies the downlink problem of a cloud-based central station (CCS) to multiple base stations (BSs) in a heterogeneous cellular network sharing the same time and frequency resources. We adopt non-orthogonal multiple access (NOMA) and propose power allocation for the wireless downlink in the heterogeneous cloud radio access network (HCRAN). Taking into account practical channel modelling with power consumptions at BSs of different cell types (e.g. macro-cell, micro-cell, etc.) and backhauling power, we analyse the energy efficiency (EE) of the practical HCRAN utilising NOMA. Simulation results indicate that the proposed NOMA for the HCRAN outperforms the conventional orthogonal frequency division multiple access (OFDMA) scheme in terms of providing higher EE of up to four times. Interestingly, the results reveal a fact that the EE of the NOMA approach is not always an increasing function of the number of BSs but varies as a quasiconcave function. This motivates us to further introduce an optimisation problem to find the optimal number of BSs that maximises the EE of the HCRAN. It is shown that, with a low power supply at the CCS, a double number of micro BSs can be served by HCRAN providing an improved EE of up to 1.6 times compared to the macro BSs and RRHs, while they achieve the same EE performance with high-power CCS.

Index Terms

Heterogeneous networks; cloud radio access networks; wireless downlink; non-orthogonal multiple access; energy efficiency.

Q.-T. Vien, T. A. Le, and B. Barn are with the School of Science and Technology, Middlesex University, United Kingdom. Email: {q.vien; t.le; b.barn}@mdx.ac.uk.

C. V. Phan is with the Department of Computer and Communications, Ho Chi Minh City University of Technology and Education, Vietnam. Email: capv@hcmute.edu.vn.

2

I. INTRODUCTION

Cloud radio access network (CRAN) has recently attracted both industrial and academic communities as a novel energy efficient architecture allowing centralised processing with collaborative radio and real-time cloud computing [1]. With the CRAN, the computational resources of all base stations (BSs) are aggregated into a virtual BS pool where a central station provides support to respective BSs with various services, such as interference management and handover control at cell boundaries [2]. The CRAN architecture is expected to not only reduce the number of cell sites but also reduce the load at the BSs while maintaining similar network coverage with BS coordination and even offering better services [1], [3]–[6]. This accordingly results in a lower energy consumption, lower capital expenditures and operating expenses.

As a promising multiple access scheme in future radio access networks, non-orthogonal multiple access (NOMA) has been proposed to improve the throughput and spectral efficiency of the downlink in wireless cellular networks [7]–[9]. The NOMA scheme allows multiple users to be laid over each other in the power domain while ensuring that all users access the shared wireless medium with the same diversity as in the conventional orthogonal multiple access technique, such as orthogonal frequency division multiple access (OFDMA). In the NOMA, successive interference cancellation (SIC) is employed at the users to recover the interested data packets resulting in not only enhanced reception capacity but also improved cell-edge user throughput [7]–[12].

Various research works have proposed the application of NOMA in different network models, such as cellular networks [7], [13]–[15] and wireless ad hoc networks [16]. However, to the best of the authors' knowledge, this work is the first attempt to investigate the NOMA and its energy efficiency in practical heterogeneous networks integrating with CRAN, namely heterogeneous

3

CRAN (HCRAN) (e.g. in [5] and references therein). In the HCRAN, BSs of various types, such as macro BSs, micro BSs, remote radio head (RRH) based BSs, pico BSs, femto BSs, etc., are incorporated via a cloud to cooperatively assist the mobile users. Such high density of BSs may cause not only severe interferences but also inefficient energy consumption.

In this paper, we first adopt NOMA for wireless downlink in HCRAN. In the proposed NOMA, the BSs of different types are allocated with different powers depending on their relative distances to the cloud-based central station (CCS) as well as the channel quality of the wireless links. Taking into account the power consumption at various BS types and the backhauling power consumption in heterogeneous network deployment, we then analyse the energy efficiency (EE)[1] of the NOMA in the practical HCRAN. It is observed that the NOMA scheme achieves a higher EE than the conventional OFDMA scheme for the HCRAN. Also, the propagation model is shown to have a considerable impact on the EE performance of both the NOMA and OFDMA schemes in practical HCRAN.

In particular, the EE of the NOMA is shown to not always increase as a function of the number of BSs. Specifically, the EE only increases when the number of BSs is less than a certain number of BSs, and then gradually decreases as the number of BSs keeps increasing. Such EE performance variance depends on many factors, such as propagation environment, power supply at the CCS and also BS types in HCRAN. Therefore, it is crucial to find the optimal number of BSs that can be served to achieve the maximal EE. To this extent, as a second contribution of the paper, we develop an algorithm to find the optimal number of BSs of various cell types based on the derived EE of the proposed NOMA. The objective is to find the number of BSs of

---

[1]The EE is defined as the ratio of the total achievable throughput and the total power consumption in the whole network, which is different from the energy per bit normalised over the transmission data rate as in [17], [18].

4

various types that can achieve the maximal EE in the practical HCRAN given the constraints on the power supply available at the CCS and the number of BSs that can be covered by the CCS. It is shown that, with a low power at the CCS, the micro BSs are more favourable to both the macro BSs and RRH-based BSs, while the same maximal EE can be achieved with either the micro BSs, macro BSs or RRH-based BSs when the power supply at the CCS is high enough.

The rest of this paper is organised as follows: Section II describes the system model of the wireless downlink in HCRAN. Section III presents the proposed NOMA and power allocation at the CSS in the HCRAN. The performance analysis of the proposed scheme is presented in Section IV where the throughput and EE of the NOMA are derived and compared with the OFDMA scheme. The EE optimisation problem is formulated in Section V to find the optimal number of BSs for maximising the EE of the wireless downlink in the HCRAN. Numerical results are presented in Section VI to validate the findings. Finally, Section VII draws the main conclusions from this paper.

II. SYSTEM MODEL OF WIRELESS BACKHAUL IN HCRAN

The system model of a HCRAN under investigation is illustrated in Fig. 1 (e.g. [5], [19]–[21]). There are K types of BSs and each k-th type, $k = 1, 2, \ldots, K$, has N_k BSs $\{\mathcal{BS}_{k,1}, \mathcal{BS}_{k,2}, \ldots, \mathcal{BS}_{k,N_k}\}$. A cloud-based central station $\mathcal{CCS}$ is employed as a central unit in the cloud to manage the whole HCRAN. The distance between the $\mathcal{BS}_{k,i_k}$, $k = 1, 2, \ldots, K$, $i_k = 1, 2, \ldots, N_k$, and the $\mathcal{CCS}$ is denoted by d_{k,i_k}. It is assumed that all the BSs $\{\mathcal{BS}_{k,i_k}\}$ are connected to the $\mathcal{CCS}$ via wireless backhaul links and the signalling between the $\{\mathcal{BS}_{k,i_k}\}$ and $\mathcal{CCS}$ is perfectly synchronised.
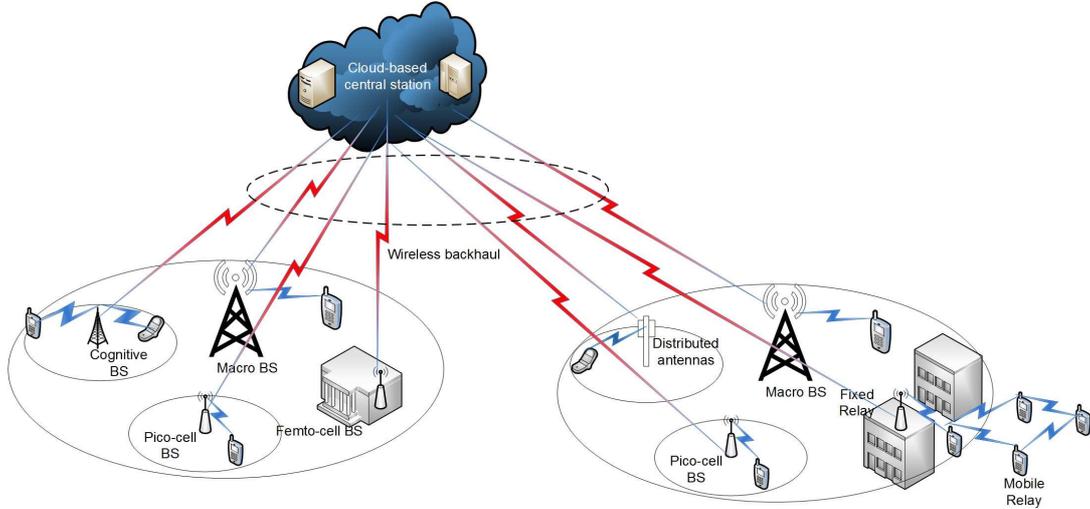
Fig. 1: System model of a HCRAN.

A. Channel Model

The wireless downlink from $\mathcal{CCS}$ to $\mathcal{BS}_{k,i_k}$, $k = 1, 2, \ldots, K$, $i_k = 1, 2, \ldots, N_k$, is assumed to suffer from flat fading h_{k,i_k} and additive Gaussian noise n_{k,i_k} having $E[|h_{k,i_k}|^2] = 1/d_{k,i_k}^{\nu_{k,i_k}}$ and $E[|n_{k,i_k}|^2] = \sigma_{k,i_k}^2$, where $E[\cdot]$ denotes the statistical expectation operation and ν_{k,i_k} ($\nu_{k,i_k} > 2$) denotes the path loss exponent of the propagation model. Let us denote W as the transmission bandwidth of the wireless downlink and P_{k,i_k} as the transmission power allocated for the $\mathcal{BS}_{k,i_k}$.

The signal transmitted from the $\mathcal{CCS}$ to $\mathcal{BS}_{k,i_k}$ is x_{k,i_k} with $E[|x_{k,i_k}|^2] = 1$. The instantaneous downlink signal-to-interference-plus-noise ratio (SINR) at the $\mathcal{BS}_{k,i_k}$, $k = 1, 2, \ldots, K$, $i_k = 1, 2, \ldots, N_k$ (i.e. γ_{k,i_k}) can be therefore given by

$$\gamma_{k,i_k} = \frac{P_{k,i_k}|h_{k,i_k}|^2}{I_{j \neq i_k} + \sigma_i^2}, \tag{1}$$

where $I_{j \neq i_k}$ represents the cumulative interference from all other BSs except the $\mathcal{BS}_{k,i_k}$.

6

B. Power Consumption Model

In a practical HCRAN shown in Fig. 1, the total power consumption in the whole network consists of not only the power consumption of the BSs but also the power consumed by the backhaul [22], [23]. In the following, we discuss about those two power-consumption modellings.

1) Power Consumption of BS: The power consumption of a BS can be modelled as in [24], [25], which includes the powers for signal processing at baseband (BB) unit, radio frequency (RF) transceiver and power amplifier (PA) as well as considering the power losses caused by DC-DC power supply, mains supply (MS), cooling and inefficiency of the PA. In this work, it is assumed that the BSs of the same type have the same power consumption. Letting $P_k^{(C)}$, $k = 1, 2, \ldots, K$, denote the power consumption of a k-th type BS, while denoting $P_k^{(A)}$, $P_k^{(RF)}$ and $P_k^{(BB)}$ as the output radiated power at an antenna element, the RF power and the BB power, respectively, we have

$$P_k^{(C)} = N_k^{(TRX)} \frac{\dfrac{P_k^{(A)}}{\eta_k^{(PA)} \left(1 - \alpha_k^{(feed)}\right)} + P_k^{(RF)} + P_k^{(BB)}}{\left(1 - \alpha_k^{(DC)}\right) \left(1 - \alpha_k^{(MS)}\right) \left(1 - \alpha_k^{(cool)}\right)}, \qquad (2)$$

where $N_k^{(TRX)}$ is the number of transceiver chains, $\eta_k^{(PA)}$ is the efficiency of the PA, $\alpha_k^{(feed)}$ is the feeder loss, $\alpha_k^{(DC)}$ is the DC-DC power supply loss, $\alpha_k^{(MS)}$ is the MS loss and $\alpha_k^{(cool)}$ is the cooling loss at the k-th type BS.

2) Backhauling Power: The power consumed by wireless backhaul for the downlink from CCS to a BS includes the power consumption at downlink interfaces of wireless switches and the power consumed by aggregation switch in the CCS. Let $P_k^{(BH)}$ denote the backhauling power of the downlink from $\mathcal{CCS}$ to a k-th type BS. Following the same approach as in [22] with the

assumption of identical downlink interfaces and switches at the BSs, $P_k^{(BH)}$ can be given by

$$P_k^{(BH)} = \frac{\omega_k P_{k,\max}^{(SW)} + (1-\omega_k)\dfrac{Ag_k^{(SW)}}{Ag_{k,\max}}P_{k,\max}^{(SW)}}{N_k^{(INT)}} + P_k^{(INT)}, \tag{3}$$

where $N_k^{(INT)}$ is the number of interfaces per switch, $P_{k,\max}^{(SW)}$ is the maximum power consumption of switch when all interfaces are used, $P_k^{(INT)}$ is the power consumption of an interface in the aggregation switch, $Ag_k^{(SW)}$ is the amount of traffic passing through the switch and $Ag_{k,\max}$ is the maximum amount of traffic that a switch at the k-th type BS can handle. Here, ω_k is a weighting factor representing the relative influence between the power consumption for the backplane of the switch (i.e. $P_{k,\max}^{(SW)}$), which is independent of the traffic and the power quantity with respect to $Ag_k^{(SW)}$ [23].

Overall, the total power consumption in the whole network can be determined by

$$P_{tot} = \sum_{k=1}^{K} \left[N_k \left(P_k^{(C)} + P_k^{(BH)} \right) + \sum_{i_k=1}^{N_k} P_{k,i_k} \right]. \tag{4}$$

III. NOMA AND POWER ALLOCATION IN HCRAN

A. Proposed NOMA for Wireless Downlink in HCRAN

In the proposed NOMA for wireless downlink in HCRAN, the signals for all BSs $\{\mathcal{BS}_{k,i_k}\}$, $k = 1, 2, \ldots, K$, $i_k = 1, 2, \ldots, N_k$, are superimposed at the $\mathcal{CCS}$ as follows

$$x = \sum_{k=1}^{K} \sum_{i_k=1}^{N_k} \sqrt{P_{k,i_k}} x_{k,i_k}. \tag{5}$$

The signal received at the $\mathcal{BS}_{k,i_k}$ over the fading channel h_{k,i_k} is therefore given by

$$y_{k,i_k} = h_{k,i_k} x + n_{k,i_k}, \tag{6}$$

where n_{k,i_k} is the complex Gaussian noise at the $\mathcal{BS}_{k,i_k}$ having zero mean and variance of σ_{k,i_k}^2.

8

At the BSs, SIC is carried out to recover the interested data in a decreasing order of the channel gain which is a function of the distance between the BSs and the CCS. In other words, the BS having a higher channel gain is decoded before the one with a lower channel gain. Let G_{k,i_k}, $k = 1, 2, \ldots, K$, $i_k = 1, 2, \ldots, N_k$, denote the normalised channel gain of the link from the $\mathcal{CCS}$ to the $\mathcal{BS}_{k,i_k}$, which is normalised by noise power as

$$G_{k,i_k} = \frac{E[|h_{k,i_k}|^2]}{\sigma_{k,i_k}^2} = \frac{1}{d_{k,i_k}^{\nu_{k,i_k}} \sigma_{k,i_k}^2}. \tag{7}$$

It can be seen in (7) that both the distance (i.e. d_{k,i_k}) and the wireless channel propagation model (i.e. ν_{k,i_k}) between $\mathcal{CCS}$ and $\mathcal{BS}_{k,i_k}$ have significant impacts on G_{k,i_k}, which affects the power allocation as well as when evaluating the EE of the wireless downlink in the HCRAN.

B. Power Allocation for Wireless Downlink in HCRAN

As noted in Section III-A, the transmitted signal power for BSs of different types should be appropriately allocated by taking into account the various distances from the BSs to the CCS along with the quality of the channels and the propagation model between them. Specifically, by using NOMA with SIC approach, the power allocated to a BS is dependent on the power of the preceding BS having higher channel gain.

Let $P_k^{(CCS)}$, $k = 1, 2, \ldots, K$, denote the total transmission power at the $\mathcal{CCS}$ for the k-type BSs, i.e.

$$P_k^{(CCS)} = \sum_{i_k=1}^{N_k} P_{k,i_k}. \tag{8}$$

For simplicity, let us assume that the noises at the BSs of the same type have the same power (i.e. $\sigma_{k,i_k}^2 = \sigma_{k,0}^2$, $\forall k = 1, 2, \ldots, K$, $i_k = 1, 2, \ldots, N_k$) and consider only the k-th type BSs. The power allocation for the whole network is straightforwardly obtained by individually treating each group of BSs of the same type.

9

Without loss of generality, let us assume that $G_{k,1} > G_{k,2} > \cdots > G_{k,N_k}$. The power allocated

at the k-th type BSs should therefore satisfy $P_{k,1} < P_{k,2} < \cdots < P_{k,N_k}$. With SIC for the NOMA,

following the same approach as in [6], let us denote τ_k ($\tau_k > 1$) as the ratio of the power allocated

for $\mathcal{BS}_{k,2}$ and the power for $\mathcal{BS}_{k,1}$. We then have

$$\tau_k = \frac{P_{k,2}}{P_{k,1}} = \frac{G_{k,1}}{G_{k,2}} \tag{9}$$

Applying recursive approach, the power allocated for $\mathcal{BS}_{k,i_k}$, $i_k = 2, 3, \ldots, N_k$, can be given by

$$P_{k,i_k} = \tau_k(\tau_k + 1)^{i_k - 2} P_{k,1}. \tag{10}$$

From (8) and (10), we obtain

$$P_k^{(CCS)} = P_{k,1} + P_{k,1}\tau_k \sum_{i_k=1}^{N_k-1} (\tau_k+1)^{i_k-1} = P_{k,1}(\tau_k+1)^{N_k-1}. \tag{11}$$

The power for $\mathcal{BS}_{k,1}$ and $\mathcal{BS}_{k,i_k}$, $i_k = 2, 3, \ldots, N_k$, can be therefore allocated as follows

$$P_{k,1} = \frac{1}{(\tau_k + 1)^{N_k - 1}} P_k^{(CCS)}, \tag{12}$$

$$P_{k,i_k} = \frac{\tau_k}{(\tau_k + 1)^{N_k - i_k + 1}} P_k^{(CCS)}. \tag{13}$$

IV. PERFORMANCE ANALYSIS

In this section, the throughput and EE of the NOMA scheme for wireless downlink in HCRAN

are derived and compared with those of the OFDMA scheme. Let us denote the total throughput

in bits/s and the EE in bits/J of scheme X, $X \in \{NOMA, OFDMA\}$, by $R^{(X)}$ and $\xi^{(X)}$,

respectively. We have

$$\xi^{(X)} \triangleq \frac{R^{(X)}}{P_{tot}}, \tag{14}$$

10

where P_{tot} is computed by (4)[2]. Therefore, in order to evaluate $\xi^{(X)}$, the total throughput achieved with each scheme (i.e. $R^{(X)}$) needs to be firstly derived.

A. Throughput & Energy Efficiency of NOMA

From (5) and (6), the signal received at $\mathcal{BS}_{k,i_k}$, $k = 1, 2, \ldots, K$, $i_k = 1, 2, \ldots, N_k$, can be rewritten as

$$y_{k,i_k} = \sum_{k=1}^{K} \sum_{i_k=1}^{N_k} h_{k,i_k} \sqrt{P_{k,i_k}} xk, i_k + n_{k,i_k}. \tag{15}$$

Therefore, the achievable throughput, in bits/s, at the $\mathcal{BS}_{k,i_k}$, $k = 1, 2, \ldots, K$, $i_k = 1, 2, \ldots, N_k$, with NOMA can be computed by

$$R_{k,i_k}^{(NOMA)} = W \log_2 \left(1 + \frac{P_{k,i_k} |h_{k,i_k}|^2}{\sum_{j=1}^{i_k-1} P_{k,j} |h_{k,j}|^2 + \sigma_k^2} \right). \tag{16}$$

The EE of NOMA for the downlink in the HCRAN can be determined by substituting (16) and (4) into (14) as

$$\xi^{(NOMA)} = \frac{\sum_{k=1}^{K} \sum_{i_k=1}^{N_k} W \log_2 \left(1 + \frac{P_{k,i_k} |h_{k,i_k}|^2}{\sum_{j=1}^{i_k-1} P_{k,j} |h_{k,j}|^2 + \sigma_k^2} \right)}{\sum_{k=1}^{K} \left[N_k \left(P_k^{(C)} + P_k^{(BH)} \right) + \sum_{i_k=1}^{N_k} P_{k,i_k} \right]}, \tag{17}$$

B. Throughput & Energy Efficiency of OFDMA

With OFDMA for wireless downlink in HCRAN, the achievable throughput, in bits/s, at the $\mathcal{BS}_{k,i_k}$, $k = 1, 2, \ldots, K$, $i_k = 1, 2, \ldots, N_k$, is simply given by

$$R_{k,i_k}^{(\text{OFDMA})} = W \beta_{k,i_k} \log_2 \left(1 + \frac{P_{k,i_k} |h_{k,i_k}|^2}{\beta_{k,i_k} \sigma_k^2} \right), \tag{18}$$

---

[2]In this work, we assume that downlink interfaces and switches are identical in both NOMA and OFDMA schemes for fair comparison of the energy efficiency and thus we assume the same total power consumption in the whole network. Although the power for data processing may be different in these two schemes, this is negligible when considering the total power consumption at the BSs.

where β_{k,i_k} denotes the ratio of bandwidth sharing satisfying $0 < \beta_{k,i_k} < 1$ and $\sum_{k=1}^{K} \sum_{i_k=1}^{N_k} \beta_{k,i_k}$ $= 1$.

The EE of OFDMA for the downlink in the HCRAN is thus given by

$$\xi^{(OFDMA)} = \frac{\sum_{k=1}^{K} \sum_{i_k=1}^{N_k} W \beta_{k,i_k} \log_2 \left(1 + \frac{P_{k,i_k} |h_{k,i_k}|^2}{\beta_{k,i_k} \sigma_k^2} \right)}{\sum_{k=1}^{K} \left[N_k \left(P_k^{(C)} + P_k^{(BH)} \right) + \sum_{i_k=1}^{N_k} P_{k,i_k} \right]}. \tag{19}$$

C. Performance comparison between NOMA and OFDMA

Let us consider an example of a HCRAN including 10 BSs of the same type[3] (i.e. $\{\mathcal{BS}_1, \mathcal{BS}_2,$ $\ldots, \mathcal{BS}_{10}\}$). Assume that user orthogonal multiplexing is combined with OFDMA. Each BS is therefore assigned a bandwidth of 0.1 Hz. It is assumed that the total available power is 100 W and the channel gains of the link between the 10 BSs and the CCS (i.e. $\{G_i\}$, $i = 1, 2, \ldots, 10$) are $\{20, 19.5, 19, 18.5, 18, 17.5, 17, 16.5, 16, 15.5\}$ dB, respectively. Here, the least channel gain is corresponding to the farthest BS (i.e. $\mathcal{BS}_{10}$), while the highest channel gain is assigned to the nearest BS (i.e. $\mathcal{BS}_1$). Following the water filling approach, the power of the 10 BSs can be allocated as $\{10.008, 10.007, 10.005, 10.004, 10.002, 10, 9.998, 9.995, 9.993, 9.99\}$ W. From (18), the data rates achieved at the 10 BSs using OFDMA scheme are $\{1.33, 1.31, 1.3, 1.28, 1.26, 1.25,$ $1.23, 1.21, 1.2, 1.18\}$ bits/sec/Hz. Thus, the total data rate with OFDMA is 12.55 bits/sec/Hz.

Using NOMA scheme, the power is allocated according to the distance between BS and CCS. Specifically, the farthest BS is allocated with the highest power and the nearest BS receives the lowest power allocation. The channel gains of the links between the 10 BSs and the CCS are assumed to be similar to the scenario with OFDMA scheme. Given a total network power of

---

[3]For simplicity, only one BS type is considered in this example to compare the performance between the NOMA and OFDMA. The usage of other BS types would also result in the same observation.

12

100 W, the power of the 10 BSs (i.e. $\{P_i\}$, $i = 1, 2, \ldots, 10$) is set as $\{0.28, 0.32, 0.54, 1.03,$ $1.95, 3.69, 6.98, 13.21, 24.99, 47.27\}$ W, respectively. Here, the power levels at the BSs are determined as in Section III-B. From (16), the data rates at the 10 BSs are $\{4.86, 2.07, 0.92,$ $0.92, 0.92, 0.92, 0.92, 0.92, 0.92, 0.92\}$ bits/sec/Hz and thus the total achievable data rate with NOMA is 14.29 bits/sec/Hz.

It can be observed in the above example that NOMA is 13.86% more efficient when compared with OFDMA considering 10 BSs. Therefore, given the same total power consumption in the whole network, the proposed NOMA also achieves a higher EE compared to the OFDMA scheme.

V. Energy Efficiency Optimisation for Wireless Downlink in HCRAN

A. Energy Efficiency Optimisation Problem

From (17), it is noticed that the EE of the NOMA scheme depends on the number of BSs of different types. In fact, as shown later in Section V-A (see Fig. 2(b)), either a very small number or a very large number of the BSs may cause a low EE, while the EE could be maximised at a certain number of the BSs. In other words, the EE does not always increase as the number of BSs increases but varies as a quasiconcave function. This accordingly means that the number of BSs needs to be determined for optimal energy efficiency performance.

For simplicity, the number of BS types (i.e. K) in HCRAN is assumed to be known and invariant. The objective of the optimisation problem is to find the optimal number of the BSs of various types to maximise the EE of the wireless downlink in the HCRAN subject to the constraints on the transmission power at $\mathcal{CCS}$ and the number of BSs of each type. The EE

13

optimisation problem can be therefore formulated as follows:

$$\max_{N_1,N_2,\ldots,N_K} \frac{\sum_{k=1}^{K}\sum_{i_k=1}^{N_k} W \log_2\left(1+\frac{P_{k,i_k}|h_{k,i_k}|^2}{\sum_{j=1}^{i_k-1}P_{k,j}|h_{k,j}|^2+\sigma_k^2}\right)}{\sum_{k=1}^{K}\left[N_k\left(P_k^{(C)}+P_k^{(BH)}\right)+\sum_{i_k=1}^{N_k}P_{k,i_k}\right]} \tag{20}$$

s.t.

$$\sum_{k=1}^{K}\sum_{i_k=1}^{N_k} P_{k,i_k} \leqslant P_{\max}^{(CCS)}, \tag{21}$$

$$N_k \leqslant N_{k,\max}, \tag{22}$$

where $P_{\max}^{(CCS)}$ denotes the maximum power available at $\mathcal{CCS}$ and $N_{k,\max}$ denotes the maximum number of k-th type BSs in the HCRAN.

B. Optimal Number of BSs

It can be observed that the optimisation problem in (20) is hard to solve directly for an exact number of BSs of different types in the whole network. Therefore, in this paper, a heuristic iteration algorithm is proposed to sequentially find the optimal number of BSs of each type. Specifically, let us consider the k-th type BSs, $k = 1, 2, \ldots, K$. The optimisation problem in (20) can be simplified as

$$\max_{N_k} \frac{\sum_{i_k=1}^{N_k} W \log_2\left(1+\frac{P_{k,i_k}|h_{k,i_k}|^2}{\sum_{j=1}^{i_k-1}P_{k,j}|h_{k,j}|^2+\sigma_k^2}\right)}{N_k\left(P_k^{(C)}+P_k^{(BH)}\right)+\sum_{i_k=1}^{N_k}P_{k,i_k}} \tag{23}$$

s.t.

$$\sum_{i_k=1}^{N_k} P_{k,i_k} \leqslant P_{k,\max}^{(CCS)} \tag{24}$$

and (22), where $P_{k,\max}^{(CCS)}$ is the maximum power allocated for the k-th type BSs at $\mathcal{CCS}$[4].

---

[4]Note that $P_{k,\max}^{(CCS)}$ depends on specific requirements and deployment in the practical network. It is further noted that $\sum_{k=1}^{K} P_{k,\max}^{(CCS)} \leqslant P_{\max}^{(CCS)}$.

14

For convenience, let us denote the objective function in (23) and the optimal number of the k-th type BSs by $\xi_k^{(NOMA)}$ and $N_{k,opt}$, respectively. The heuristic iteration algorithm for finding the optimal number of BSs of various types in the HCRAN is summarised in Algorithm 1.

Algorithm 1 Optimal Number of BSs for Maximal EE in HCRAN

1: **for** $k = 1$ to K **do**

2:     $N_{k,opt} \leftarrow 0$

3:     $\xi_{k,\max}^{(NOMA)} \leftarrow 0$

4:     **for** $j = 1$ to $N_{k,\max}$ **do**

5:         Find $\{P_{k,i_k}\}$, $i_k = 1, 2, \ldots, j$, using (12) and (13).

6:         Find $\xi_k^{(NOMA)}$ in (23).

7:         **if** $\xi_k^{(NOMA)} \geqslant \xi_{k,\max}^{(NOMA)}$ **then**

8:             $N_{k,opt} \leftarrow j$

9:             $\xi_{k,\max}^{(NOMA)} \leftarrow \xi_k^{(NOMA)}$

10:         **else**

11:             **break**

12:         **end if**

13:     **end for**

14: **end for**

15

VI. NUMERICAL RESULTS

This section shows the numerical results of EE[5] achieved with the proposed NOMA for wireless downlink in HCRAN as well as indicating the optimal number of BSs for maximising the EE with the proposed heuristic iteration searching algorithm. The simulations are carried out in MATLAB for different values of path loss exponents (i.e. ν) to characterise practical propagation environments. Specifically, two scenarios of $\nu = 2.4$ and $\nu = 3$ are considered to represent urban and shadowed urban (or suburban) cellular radio environment, respectively.

Three BS types are investigated (i.e. $K = 3$) including macro, RRH and micro BSs. For simplicity, the BSs are assumed to be sequentially located with respect to the position of $\mathcal{CCS}$. This means the macro BSs are nearer to the $\mathcal{CCS}$ than the RRH, while the micro BSs are located furthest from the $\mathcal{CCS}$. For power consumption modelling, using (2) with simulation parameters for BSs as in [24], the power consumption of macro, RRH and micro BSs can be determined as $P_1^{(C)} = 1350$ W, $P_2^{(C)} = 754.8$ W and $P_3^{(C)} = 144.6$ W, respectively. Regarding the backhaul, as in [22], we assume that there are 24 interfaces per switch, the maximum power consumption of a switch is 300 W, the power consumption of a downlink interface in the aggregation switch is 1 W, weighting factor is 0.5, the amount of traffic passing through the switch is 1 Gbits/s and the maximum amount of traffic that a switch can handle is 24 Gbits/s.

A. NOMA versus OFDMA in relation to Propagation Models

Figures 2(a) and 2(b) sequentially illustrate the achievable total throughput and EE of the downlink in HCRAN using the proposed NOMA and that of the conventional OFDMA scheme.
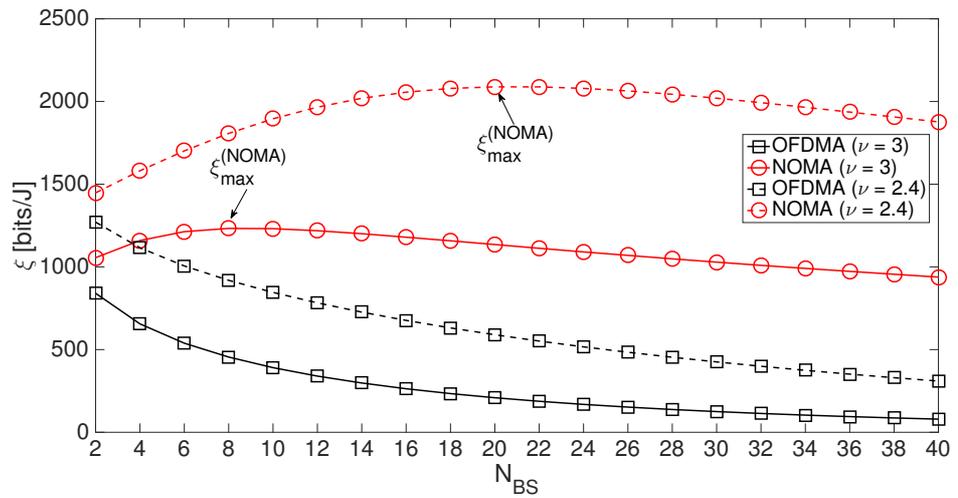
[5]Note that the numerical results in this Section are generated by Monte Carlo simulation over a number of channel realisations using the derived expressions in Section IV.

16
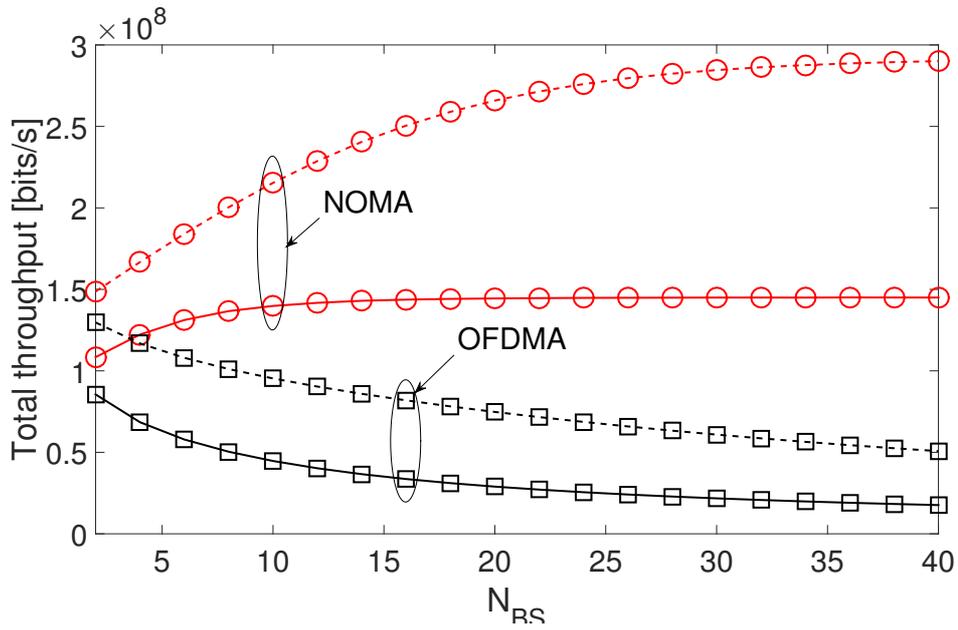
(a)

(b)

Fig. 2: (a) Total throughput and (b) EE of NOMA and OFDMA schemes w.r.t. various propagation path loss exponents.

Both the total throughput and EE are plotted as functions of the number of BSs which is assumed to vary in the range of 2 to 40 BSs. It is assumed that the distances between the BSs and $\mathcal{CCS}$ are in the range of 100 m to 8 km with an interval of 200 m corresponding to the channel gain from 20 dB to 0 dB with a decrement factor of $-1/2$, the total transmission power at the $\mathcal{CCS}$ is 100 kW and the transmission bandwidth is 10 MHz. It can be observed in Fig. 2 that the proposed NOMA achieves higher throughput and higher EE compared to the OFDMA scheme. Specifically, the throughput and EE gains of the NOMA are approximately up to 3 times and up to 4 times, respectively, higher than that of the OFDMA. This accordingly verifies the better performance achieved with the proposed NOMA for the wireless downlink in HCRAN.

In Fig. 2(a), it is noted that, with the increase in the number of BSs in NOMA scheme, there is an increase in the throughput up to a certain level, referred to as the maximum achievable throughput. Further increase in the number of BSs will maintain the same throughput. Specifically, in the considered scenario, the NOMA achieves a maximum throughput of 300 Mbits/sec when $\nu = 2.4$, while 145 Mbits/sec when $\nu = 3$. This implies that the total power available is sufficient to maintain a high efficiency for a certain number of BSs. Also, considering the impact of the wireless propagation environment in Fig. 2, the throughput and EE of the NOMA in the urban area (i.e. $\nu = 2.4$) are shown to be achieved as twice as that in the suburban area (i.e. $\nu = 3$). In fact, the higher the path loss factor is, the less the performance can be achieved.

Furthermore, it can be noticed in Fig. 2(b) that the EE of the NOMA does not always increase as the number of BSs increases, but varies as a quasiconcave function. For example, the EE only increases when the number of BSs is less than 20 BSs and 8 BSs when $\nu = 2.4$ and $\nu = 3$, respectively, and then gradually decreases as the number of BSs keeps increasing. This accordingly implies that the EE of the NOMA can be maximised at a certain number of BSs

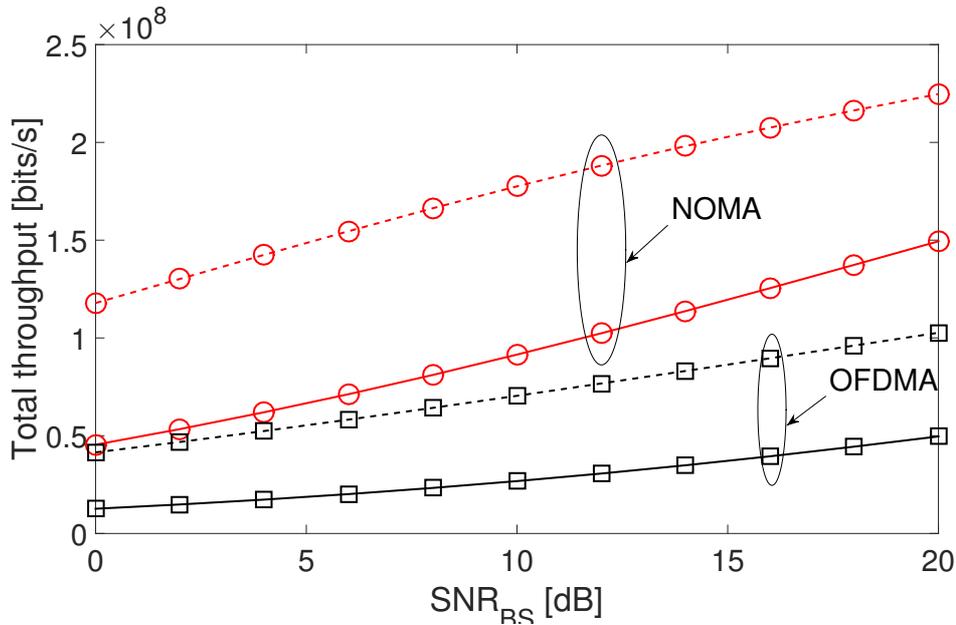depending on the propagation models.

B. Impact of Channel Quality

Fig. 3: Total throughput of NOMA and OFDMA schemes over SNR of BS.

Taking into account the impact of the SNR of the BSs on the throughput performance of the wireless downlink in HCRAN, Fig. 3 plots the total throughput of NOMA and OFDMA schemes as functions of the SNR with respect to different radio environments (i.e. $\nu = 3$ and $\nu = 2.4$). It is assumed that there are 10 macro BSs in the HCRAN and the total available power is 100 kW. In Fig. 3, the NOMA scheme is shown to achieve a higher throughput than OFDMA scheme for all range of the SNRs. For example, for an SNR value of 20 dB, the NOMA achieves up to three times increase in the total throughput when compared to the OFDMA scheme. It is also noted in both the schemes that the total throughput increases as the SNR of the BSs increases. However, the performance slope of the NOMA scheme is much steeper, which again validates

the superiority of the NOMA over the OFDMA scheme.
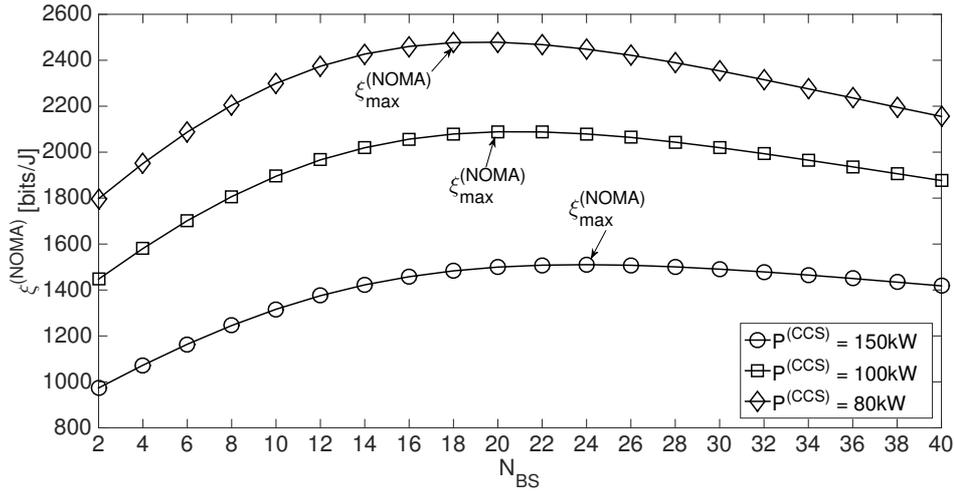
C. Impact of Power Allocation at $\mathcal{CCS}$

Fig. 4: EE of NOMA w.r.t. various power allocated at $\mathcal{CCS}$.

Investigating the impact of power allocation at $\mathcal{CCS}$ on the performance of the proposed NOMA for wireless downlink in HCRAN, Fig. 4 plots the EE versus the number of BSs with respect to different values of power supply available at the $\mathcal{CCS}$ (i.e. $P^{(CCS)}$). Specifically, three scenarios of $P^{(CCS)} = \{150, 100, 80\}$ kW are considered for urban cellular network model with $\nu = 2.7$. With similar settings as in Fig. 2(b), it can be observed that, as long as the $\mathcal{CCS}$ is able to support the BSs, only a low power is required at the $\mathcal{CCS}$, and thus results in the highest EE performance. In fact, it can be noticed from (16) that the total throughput is not considerably changed as the total power at $\mathcal{CCS}$ increases. Therefore, further increasing $P^{(CCS)}$ results in a lower EE. Additionally, the maximal performance is shown to be achieved at a specific number of BSs according to the power available at the $\mathcal{CCS}$.
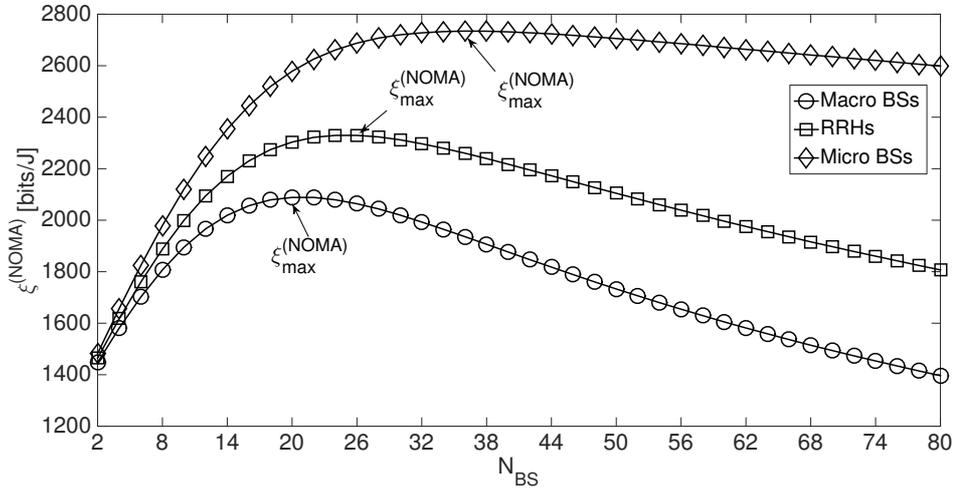
D. Impact of BS Types

Fig. 5: EE of NOMA w.r.t. various BS types.

Taking into account the impact of the BS types on the EE of the wireless downlink in HCRAN, Fig. 5 plots the EE of the NOMA for three BS types including macro BSs, RRH and micro BSs. The simulation parameters are similarly set as in Fig. 2(b) for urban cellular model with $\nu = 2.7$. In Fig. 5, the deployment of micro BSs is shown to achieve the best EE performance, especially in a large network, while the same EE can be achieved with any BS types in a small network. In fact, this is due to the difference in power consumption at the BSs of different types. It is also noted in Fig. 5 that the number of BSs for maximising the EE is related to the BS types.

E. Optimal Number of BSs in HCRAN

Figures 6(a) and 6(b) sequentially plot the optimal number of BSs (i.e. N_{opt}) using the proposed Algorithm 1 and the corresponding maximal EE (i.e. $\xi_{\max}^{(NOMA)}$) as functions of the maximum
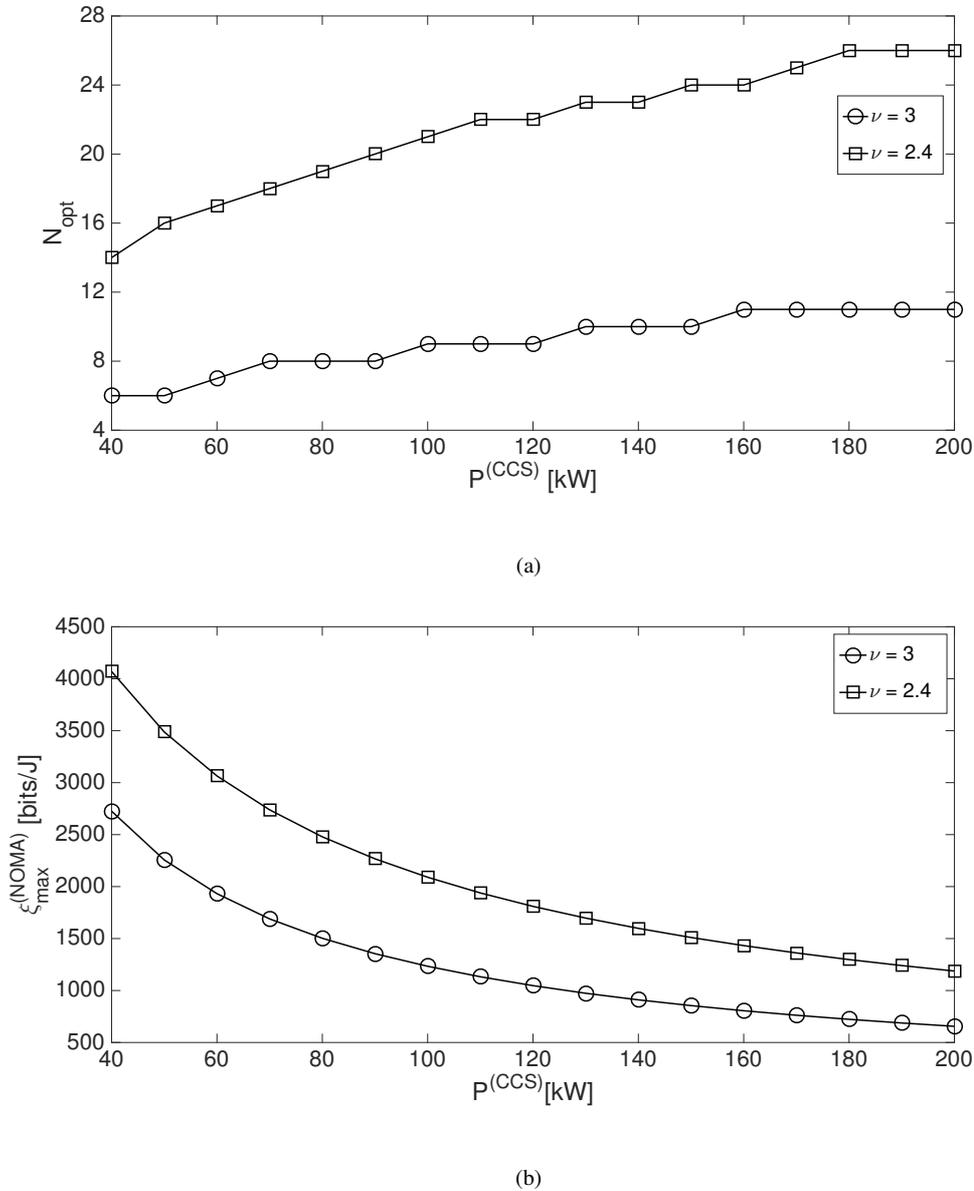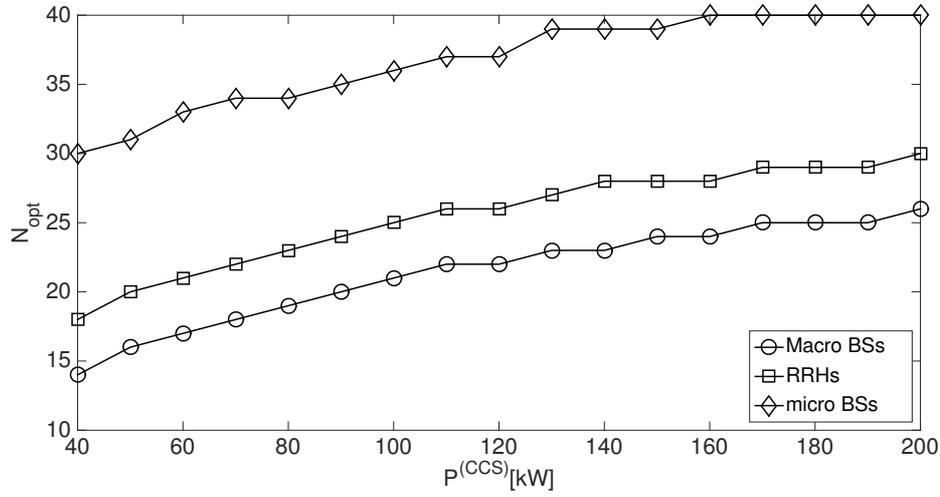
(a)

(b)

Fig. 6: (a) Optimal number of BSs versus maximum power and (b) Maximal EE versus maximum power at $\mathcal{CCS}$ w.r.t. various propagation path loss exponents.

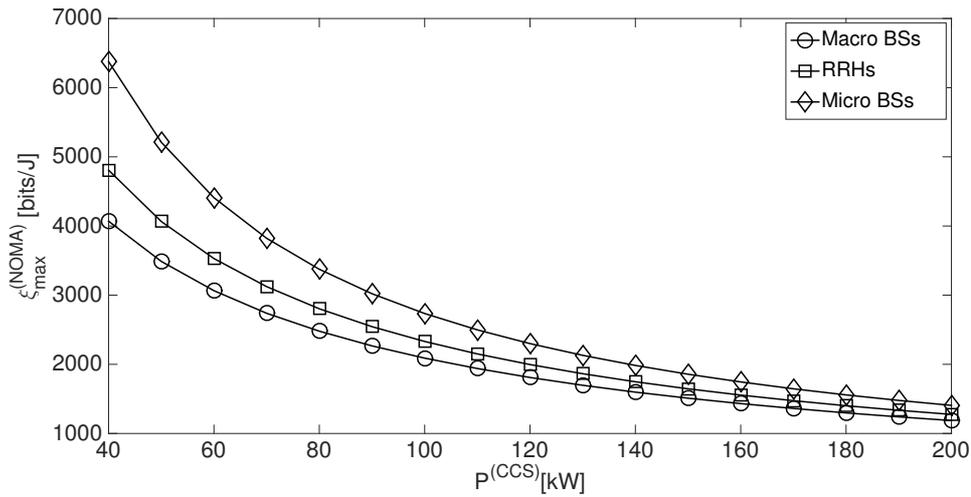power available at $\mathcal{CCS}$ (i.e. $P_{\max}^{(CCS)}$). Urban and suburban cellular propagation models with $\nu = 2.7$ and $\nu = 3$ are considered. The other simulation parameters are similarly set as in Fig. 2.

(a)

(b)

Fig. 7: (a) Optimal number of BSs versus maximum power and (b) Maximal EE versus maximum

power at $\mathcal{CCS}$ w.r.t. various BS types.

It can be observed that the optimal number of BSs increases as the power at $\mathcal{CCS}$ increases. In

addition, the urban model is shown to be able to support more BSs with a higher peak of EE

compared to the suburban propagation model.

Considering different BS types in HCRAN, Figs. 7(a) and 7(b) plot N_{opt} and $\xi_{\max}^{(NOMA)}$, respectively, versus $P_{\max}^{(CCS)}$ for three BS types (i.e. macro BSs, RRHs and micro BSs) with the same simulation parameters as in Fig. 5. It can be seen that, with a low power at the $\mathcal{CCS}$, a double optimal number of the micro BSs can be supported for a higher EE of up to 1.6 times compared to the macro BSs and RRHs. On the other hand, when the power supply at the $\mathcal{CCS}$ is high, the same maximal EE is shown to be achieved with either the macro BSs, RRHs or micro BSs.

VII. Conclusions

In this paper, an efficient NOMA scheme has been proposed for wireless downlink in practical HCRAN. A power allocation scheme has been developed to allocate the power at the BSs of different types. It has been shown that the proposed NOMA achieves an improved EE performance of up to four times over the conventional OFDMA scheme. Furthermore, a heuristic iteration search algorithm has been developed to find the optimal number of BSs of every type to maximise the EE of the HCRAN taking into account the practical channel modelling, power consumption at various BS types and backhauling power consumption. With a low power supply at the CCS, a double number of micro BSs with an improved EE of up to 1.6 times has been shown to be achieved compared to the macro BSs and RRHs, while the high-power CCS has been indicated to be able to support all BS types with the same EE performance. For future work, we will derive the closed-form expressions for the averaged total throughput and EE of the proposed NOMA.

24

REFERENCES

[1] J. Wu, Z. Zhang, Y. Hong, and Y. Wen, "Cloud radio access network (C-RAN): a primer," *IEEE Netw.*, vol. 29, no. 1, pp. 35–41, Jan. 2015.

[2] White Paper, "C-RAN: The road towards green RAN," China Mobile Labs, Ver. 3.0, Dec. 2013.

[3] Z. Ding and H. Poor, "The use of spatially random base stations in cloud radio access networks," *IEEE Signal Process. Lett.*, vol. 20, no. 11, pp. 1138–1141, Nov. 2013.

[4] K. Sundaresan, M. Y. Arslan, S. Singh, S. Rangarajan, and S. V. Krishnamurthy, "Fluidnet: A flexible cloud-based radio access network for small cells," in *Proc. ACM MobiCom 2013*, Miami, Florida, USA, Sep. 2013, pp. 99–110.

[5] M. Peng, Y. Li, J. Jiang, J. Li, and C. Wang, "Heterogeneous cloud radio access networks: a new perspective for enhancing spectral and energy efficiencies," *IEEE Wireless Commun. Mag.*, vol. 21, no. 6, pp. 126–135, Dec. 2014.

[6] Q.-T. Vien, N. Ogbonna, H. X. Nguyen, R. Trestian, and P. Shah, "Non-orthogonal multiple access for wireless downlink in cloud radio access networks," in *Proc. IEEE EW 2015*, Budapest, Hungary, May 2015, pp. 434–439.

[7] Z. Ding, Z. Yang, P. Fan, and H. Poor, "On the performance of non-orthogonal multiple access in 5G systems with randomly deployed users," *IEEE Signal Process. Lett.*, vol. 21, no. 12, pp. 1501–1505, Dec. 2014.

[8] A. Benjebbour, Y. Saito, Y. Kishiyama, A. Li, A. Harada, and T. Nakamura, "Concept and practical considerations of non-orthogonal multiple access (NOMA) for future radio access," in *Proc. ISPACS 2013*, Okinawa, Japan, Nov. 2013, pp. 770–774.

[9] Y. Saito, Y. Kishiyama, A. Benjebbour, T. Nakamura, A. Li, and K. Higuchi, "Non-orthogonal multiple access (NOMA) for cellular future radio access," in *Proc. IEEE VTC 2013-Spring*, Dresden, Germany, Jun. 2013, pp. 1–5.

[10] H. Osada, M. Inamori, and Y. Sanada, "Non-orthogonal access scheme over multiple channels with iterative interference cancellation and fractional sampling in MIMO-OFDM receiver," in *Proc. IEEE VTC 2013-Fall*, Las Vegas, USA, Sep. 2013, pp. 1–5.

[11] N. Otao, Y. Kishiyama, and K. Higuchi, "Performance of non-orthogonal access with SIC in cellular downlink using proportional fair-based resource allocation," in *Proc. ISWCS 2012*, Paris, France, Aug. 2012, pp. 476–480.

[12] H. Osada, M. Inamori, and Y. Sanada, "Non-orthogonal access scheme over multiple channels with iterative interference cancellation and fractional sampling in OFDM receiver," in *Proc. IEEE VTC 2012-Spring*, Yokohama, Japan, May 2012, pp. 1–5.

[13] Z. Ding, M. Peng, and H. Poor, "Cooperative non-orthogonal multiple access in 5g systems," *IEEE Commun. Lett.*, vol. 19, no. 8, pp. 1462–1465, Aug 2015.

25

[14] J. Men and J. Ge, "Performance analysis of non-orthogonal multiple access in downlink cooperative network," *IET Commun.*, vol. 9, no. 18, pp. 2267–2273, 2015.

[15] Y. Saito, A. Benjebbour, Y. Kishiyama, and T. Nakamura, "System-level performance evaluation of downlink non-orthogonal multiple access (NOMA)," in *Proc. IEEE PIMRC 2013*, London, UK, Sep. 2013, pp. 611–615.

[16] J. Choi, "On multiple access using H-ARQ with SIC techniques for wireless ad hoc networks," *Wireless Pers. Commun.*, vol. 69, no. 1, pp. 187–212, 2013.

[17] Q.-T. Vien, B. G. Stewart, J. Choi, and H. X. Nguyen, "On the energy efficiency of HARQ-IR protocols for wireless network-coded butterfly networks," in *Proc. IEEE WCNC 2013*, Shanghai, China, Apr. 2013, pp. 2559–2564.

[18] Q.-T. Vien, H. X. Nguyen, B. G. Stewart, J. Choi, and W. Tu, "On the energy-delay tradeoff and relay positioning of wireless butterfly networks," *IEEE Trans. Veh. Technol.*, vol. 64, no. 1, pp. 159–172, Jan. 2015.

[19] X. Peng, J. C. Shen, J. Zhang, and K. B. Letaief, "Joint data assignment and beamforming for backhaul limited caching networks," in *Proc. IEEE PIMRC 2014*, Washington, DC, USA, Sep. 2014, pp. 1370–1374.

[20] A. Benjebbour, M. Shirakabe, Y. Ohwatari, J. Hagiwara, and T. Ohya, "Evaluation of user throughput for mu-mimo coordinated wireless networks," in *2008 IEEE 19th International Symposium on Personal, Indoor and Mobile Radio Communications*, Cannes, France, Sep. 2008, pp. 1–5.

[21] T. A. Le and M. R. Nakhai, "Throughput analysis of network coding enabled wireless backhauls," *IET Commun.*, vol. 5, no. 10, pp. 1318–1327, July 2011.

[22] S. Tombaz, P. Monti, K. Wang, A. Vastberg, M. Forzati, and J. Zander, "Impact of backhauling power consumption on the deployment of heterogeneous mobile networks," in *Proc. IEEE GLOBECOM 2011*, Houston, TX, USA, Dec. 2011, pp. 1–5.

[23] O. Onireti, F. Heliot, and M. Imran, "On the energy efficiency-spectral efficiency trade-off of distributed MIMO systems," *IEEE Trans. Commun.*, vol. 61, no. 9, pp. 3741–3753, Sep. 2013.

[24] G. Auer, V. Giannini, C. Desset, I. Godor, P. Skillermark, M. Olsson, M. Imran, D. Sabella, M. Gonzalez, O. Blume, and A. Fehske, "How much energy is needed to run a wireless network?" *IEEE Wireless Commun. Mag.*, vol. 18, no. 5, pp. 40–49, Oct. 2011.

[25] B. H. Jung, H. Leem, and D. K. Sung, "Modeling of power consumption for macro-, micro-, and RRH-based base station architectures," in *Proc. IEEE VTC 2014-Spring*, Seoul, Korea, May 2014, pp. 1–5.